ChemPubSoc Europe

DOI: 10.1002/cmdc.201700466

CHEMMEDCHEM Full Papers

Encapsulating Active Pharmaceutical Ingredients in Self-Assembling Adamantanes with Short DNA Zippers

Helmut Griesser, Alexander Schwenger, and Clemens Richert*[a]

Dedicated to Wolfgang Pfleiderer on the occasion of his 90th birthday.

Formulating pharmaceutically active ingredients for drug delivery is a challenge. There is a need for new drug delivery systems that take up therapeutic molecules and release them into biological systems. We propose a novel mode of encapsulation that involves matrices formed through co-assembly of drugs with adamantane hybrids that feature four CG dimers as sticky ends. Such adamantanes are accessible via inexpensive solution-phase syntheses, and the resulting materials show attractive properties for controlled release. This is demonstrated for two different hybrids and a series of drugs, including anticancer drugs, antibiotics, and cyclosporin. Up to 20 molar equivalents of active pharmaceutical ingredients (APIs) are encapsulated in hybrid materials. Encapsulation is demonstrated for DNA-binding and several non-DNA binding compounds. Nanoparticles were detected that range in size from 114–835 nm average diameter, and ζ potentials were found to be between −29 and +28 mV. Release of doxorubicin into serum at near-constant rates for 10 days was shown, demonstrating the potential for slow release. The encapsulation and release in self-assembling matrices of dinucleotide-bearing adamantanes appears to be broadly applicable and may thus lead to new drug delivery systems for APIs.

Introduction

Formulating active pharmaceutical ingredients (APIs) with unfavorable physicochemical properties in drug delivery systems is important to achieve the desired absorption, distribution and duration of the therapeutic effect.[1] Pharmaceutical carriers can also improve tissue selectivity and can thus decrease side effects. The search for formulations is therefore an active area of research, and new solutions for drug delivery challenges are being sought. This includes the development of drug delivery vehicles based on liposomes, polymeric micelles,[2] lipid nanoparticles,[3] or biomacromolecules, such as proteins or nucleic acids.[4–8]

One class of pharmaceutically active compounds for which new carrier systems are being developed is the class of anthracyclines. Anthracyclines are chemotherapeutic agents from Streptomyces bacteria that are used extensively as anticancer therapeutics in the clinic.[9] Among the cancers that are being treated with anthracyclines are bladder, breast, lung and ovarian cancers, leukemias and lymphomas.[10] Their mode of action continues to be studied, both experimentally and with computational methods.[11] The better known anthracyclines include daunorubicin, doxorubicin, its epimer epirubicin and idarubicin. A liposomal nanocarrier for doxorubicin was approved by the FDA in 1995 and was marketed for the treatment of Kaposi's sarcoma or ovarian cancer under the drug name Doxil. The drug Lipodox is marketed as a close derivative of Doxil.[12] Experimental drug delivery systems for doxorubicin include formaldehyde conjugates,[13] protein cages,[14] metal organic frameworks,[15] HPMA copolymers[16] and DNA-PEG conjugates.[17] A recent DNA nanocarrier for doxorubicin was shown to have tunable release properties.[18] Nanoscale DNA constructs have also been used for formulating daunorubicin to circumvent drug resistance.[19] Some of these results suggested that DNA-based structures are suitable as carriers for anthracyclines.

Unfortunately, long oligonucleotides or nucleic acids can be difficult and expensive to produce, requiring either solid-phase syntheses or complex biotechnological processes.[20] Further, long linear DNA does not readily form cavities of a size suitable for encapsulating small molecules with high efficiency. Nor do the complex multistrand assemblies typically produced with the DNA origami technique[21,22] lend themselves to scale-up for producing the quantities required for clinical studies. Instead, a new class of oligonucleotide-based compounds that was developed in the realm of DNA nanotechnology seemed more promising. This is the class of branched oligonucleotide hybrids,[23] whose ability to form three-dimensional networks with small cavities via hybridization, combined with the tunability of the interaction strength through changes in the sequence and length of the DNA chains, and the biodegradable nature of their DNA arms makes them unique among the novel bio-based materials.

[a] H. Griesser, A. Schwenger, Prof. C. Richert
Institute of Organic Chemistry, University of Stuttgart, Pfaffenwaldring 55, 70569 Stuttgart (Germany)
Fax: (+49) 0711-685-64321
E-mail: lehrstuhl-2@oc.uni-stuttgart.de

Supporting information and the ORCID identification number(s) for the author(s) of this article can be found under: https://doi.org/10.1002/cmdc.201700466.

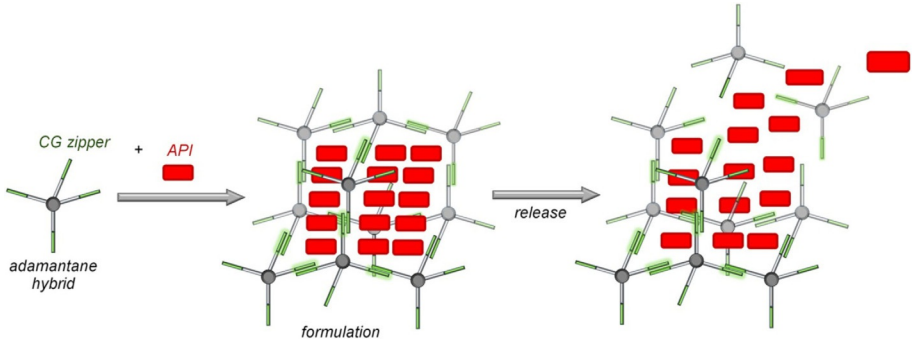

Figure 1. Formulation and release of an active pharmaceutical ingredient with an adamantane hybrid with CG dimers as DNA zipper arms.

We had recently reported branched oligonucleotide hybrids, consisting of very short DNA arms and an organic branching element as core.[23] Because of multivalent interactions, dinucleotide arms of the sequence 5′-CG-3′ suffice to induce the formation of materials upon hybridization of hybrids with four, six or eight arms in aqueous buffer containing magnesium ions.[24,25] Efficient and scalable solution-phase syntheses make these compounds available at a fraction of the cost of linear oligonucleotides.[26,27] Uptake of DNA staining agents demonstrated that the three-dimensional networks can accommodate guest molecules in the solids formed upon hybridization,[24,27] but it was unclear whether drugs would be incorporated. This prompted us to test whether hybrids with CG zipper arms can act as matrix for the formulation of APIs.

Herein we report that branched oligonucleotide hybrids with CG zipper arms take up significant quantities of APIs, forming inclusion compounds from aqueous solutions (Figure 1). This was first shown for anthracyclines, and was then extended to other pharmacologically active agents, including Gleevec. Exploratory work shows that from the inclusion compounds, the API can be released into biological fluids at body temperature. The formulation of doxorubicin contains up to 12 molar equivalents of the drug over the adamantane and has attractive release properties, with near-constant rates of drug release into serum over ten days in an in vitro model system.

Results and Discussion

Figure 2 shows the structure of the branched oligonucleotides that were used to formulate the anthracyclines. Two different adamantane cores were used. The first is the tetrakis(*p*-hydroxybiphenyl)adamantane (TBA) core,[27] with stiff spacers between the adamantane branching element and the DNA arms. The second core dubbed "TOA" features just the four hydroxy groups of adamantane tetraol as the attachment points for the DNA arms and was designed to form more hydrophilic lattices with smaller cavities.[28] We expect the short DNA arms to be fully biodegradable by nucleases in the body, without producing toxic metabolites. Substituted adamantanes are known as lead structures in medicinal chemistry,[29] and even aminoadamantanes, such as amantadine,[30] rimantadine[31] or adapromine,[32] have been approved as drugs, with acceptable toxicity

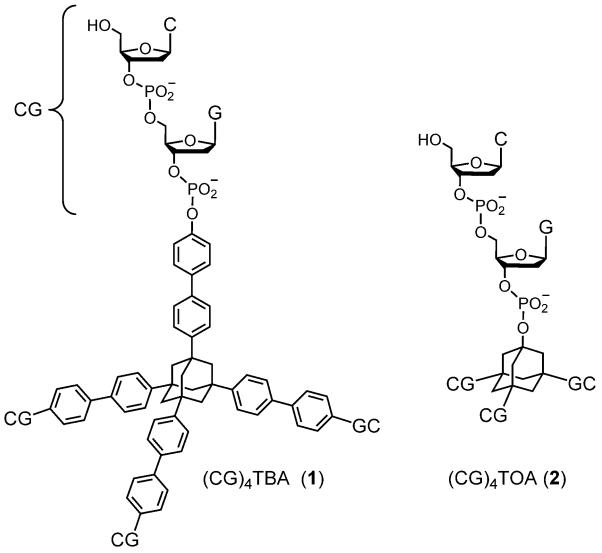

Figure 2. Structure of adamantane hybrids $(CG)_4$TBA (**1**) and $(CG)_4$TOA (**2**) with CG zipper arms.

profiles. The same is true for kemantane, a hydroxyketone derivative of adamantane that is metabolized to a diol.[32] Adamantane tetraol, the final product of nuclease digestion, is an aliphatic alcohol for which, to the best of our knowledge, no special toxicity has been reported.

As mentioned above, we wished to study whether APIs can be encapsulated with DNA-bearing adamantanes that assemble via base pairing, prompting us to include a broad range of different structures. Figure 3 gives an overview of the APIs studied.

The first series of formulations were prepared with $(CG)_4$TBA (**1**). For this, a solution of the hybrid in 10 mM acetate buffer was heated to 80 °C, allowed to cool, and treated with a solution of the active pharmaceutical ingredient while at 60 °C, followed by cooling the resulting mixture to 20 °C in 12 h. Figure 4 shows representative photographs of solids formed with anthracyclines. The solids were isolated by centrifugation and washed once with water. The amount of remaining API and hybrid carrier were determined in the mother liquor via absorption spectroscopy, and a sample of the solid was dissolved and also analyzed. Further, control experiments were performed in every case, in which the API solution was treated

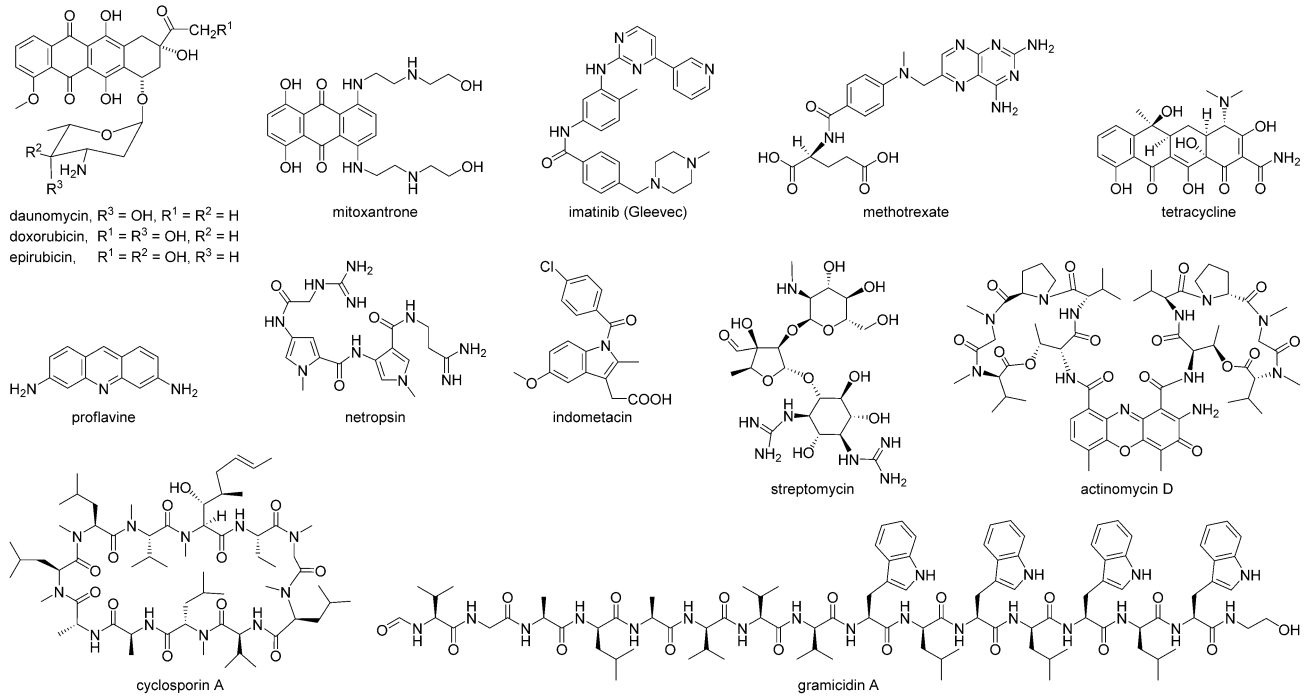

Figure 3. Structures of small- and medium-size APIs used in this study.

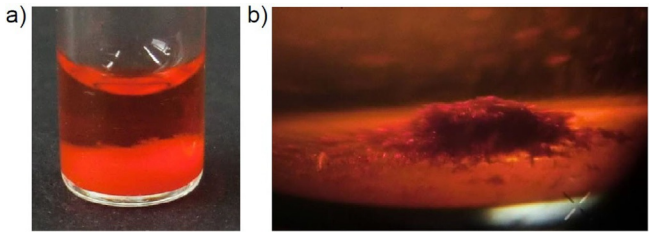

Figure 4. Photographs of samples of compounds formed from hybrids and anthracyclines in 10 mM aqueous NH_4OAc buffer after 1 d at 22 °C. a) $(CG)_4TBA$ (125 μM) treated with daunomycin (1.25 mM), with the material visible at the bottom of the glass vial. b) Microscopic image of the solid formed from a sample of $(CG)_4TBA$ (125 μM) and doxorubicin (1.88 mM) produced using the same protocol.

with water, rather than the hybrid solution. Only in three cases (doxorubicin, epirubicin and tetracycline) were small quantities of a precipitate ($\leq$20%) found in the control assay upon cooling for up to 3 d. Table 1 gives an overview of the results of the assays producing the inclusion compounds.

Either of the three anthracycline APIs tested (daunomycin, doxorubicin and epirubicin) gave a solid, with quantitative precipitation of **1** from the buffer. Up to twelve equivalents of the antibiotics were found in the formulation, which for doxorubicin equals 66% of the dry weight of the preparation (not considering counterions and hydration). This encouraged us to test other compound classes. First, we formulated other compounds known to interact with DNA, including proflavine and mitoxantrone, two intercalators, and netropsin, a minor groove binder. Either of the drugs was encapsulated well, with $\geq$5 molar equivalents of the API over the carrier included in the solid (Table 1).

The ability of hybrid **1** to form inclusion compounds is not limited to drugs known to act on nucleic acids. Imatinib, better known under its trade name Gleevec, a kinase inhibitor and important anticancer medication, was also formulated when combined with **1** in hot aqueous solution, with eight equivalents encapsulated in the inclusion compound, which was often initially oily or glassy for this API. Also, a number of antibiotics was converted into solid inclusion complexes when treated with **1** in the presence of 10 mM magnesium chloride. This included tetracycline, a protein biosynthesis inhibitor binding to bacterial ribosomes, of which five equivalents were found in the compound formed with **1**, and streptomycin, an aminoglycoside and one of the WHOs "essential medicines" (Table 1). The latter does not intercalate and does not feature a chromophore, so that it was hard to quantify by absorbance measurements. So, uptake of the API in the solid was confirmed by TLC. In the preparation, the precipitation of **1** was again near-quantitative according to UV-absorbance.

An antibiotic of vastly different structure and mode of action, gramicidin A, was also incorporated in a solid formed with **1** at 10 mM $MgCl_2$. Here, ethanol had to be used in the preparation to ensure sufficient initial solubility of the linear pentadecapeptide, known to act as pore-forming membrane channel in bacteria. It is not surprising that just half an equivalent of gramicidin was incorporated, given its molecular weight of almost 2 kDa. We were surprised and encouraged to see that even cyclosporin, an immunosuppressant that is also on the WHO's list of the most effective and safe medicines in the health system that acts on protein targets, formed an equimolar inclusion complex with **1** when formulated with the aid of 25% ethanol. Further, methotrexate, an antifolate anticancer agent and immunosuppressant formed a roughly equimolar in-

Table 1. Formation of inclusion compounds from $(CG)_4TBA$ (**1**) and active pharmaceutical ingredients (APIs) from dilute aqueous buffer.[a]

Concentration of **1**	API (equiv)	conc. $MgCl_2$ [mM]	λ_{det} API [nm]	Hybrid precipitated [%]	Inclusion efficiency (molar ratio: API/hybrid)
250 μM	daunomycin (10)	–	487	>95	8:1
50 μM	daunomycin (10)			>95	8:1
250 μM	doxorubicin (15)	–	487	>95	12:1
50 μM	doxorubicin (15)			>95	13:1
50 μM	epirubicin (15)	–	485	>95	12:1
50 μM	proflavine (15)	–	442	>95	8:1
	proflavine (27)			>95	10:1
50 μM	mitoxantrone (15)	–	610	90	5:1
50 μM	netropsin (15)	–	296	>95	6:1
50 μM	imatinib (15)	–	335	>95[b]	8:1
50 μM	tetracycline (18)	10	360	90	5:1
50 μM[c]	streptomycin (5)	10	–	>95	$c_{sol} < c_0$[d]
50 μM	methotrexate (15)	10	373	90	1:1
1 mM	methotrexate (4)	10		90	1.2:1
50 μM in buffer/EtOH (1:1)[c]	gramicidin A (3)	10	282	>95	0.5:1[e]
50 μM in buffer/EtOH (3:1)[c]	cyclosporin A (3)	10	229	>95	1:1[f]
50 μM	actinomycin D (7.5)	100	440	no solid	–[g]
50 μM[c]	cytochrome c (5)	10	410	30	<0.05:1
		100		>95	<0.05:1

[a] Conditions: 10 mM NH_4OAc buffer, pH 7, mixing at 70 °C, cooling to room temperature within 12 h. All APIs, except gramicidin A and cyclosporin A, were well soluble in water and were added as aliquots of 0.5–10 mM stock solutions. [b] Depending on the temperature, an oily or glassy product was obtained. [c] Mixed at 22 °C. [d] More API in solid than in solution, as detected by TLC. [e] Presence of hybrid and API in solid confirmed by MALDI-TOF MS, *m/z* 3282 (**1**) and $[M+H]^+$ 1881 (gramicidin). [f] Presence of hybrid and API in solid confirmed by MALDI-TOF MS of analytical sample, *m/z* $[M-H]^-$ 3282 (hybrid); and $[M+H]^+$ 1203 (cyclosporin). [g] This API appears to inhibit precipitation of carrier; no solid at 0, 10, or 100 mM $MgCl_2$.

clusion complex with DNA hybrid **1** at low $MgCl_2$ concentration, with 90% of **1** being found in the solid at room temperature.

On the other hand, actinomycin D, also known as Dactinomycin, a transcriptional inhibitor that binds to the transcription initiation complex, did not form an solid when combined with **1** in aqueous buffer, even when up to 100 mM $MgCl_2$ was added. Because such a high concentration of magnesium ions usually induces the precipitation of the hybrid,[23,24] this suggests that the known DNA-binder can suppress the formation of the insoluble three-dimensional network of the hybrid. Not surprisingly, cytochrome c, a hemeprotein involved in respiratory chain redox reactions in mitochondria of over 100 amino acid residues does not form an inclusion material with $(CG)_4TBA$ (**1**), but it also does not inhibit material formation at high magnesium concentration. Here, the large and well-soluble potential guest molecule remains in solution when the hybrid forms an insoluble 3D network (last entry of Table 1).

We then tested the smaller adamantane tetraol-based hybrid **2** for its ability to form inclusion compounds with dox-

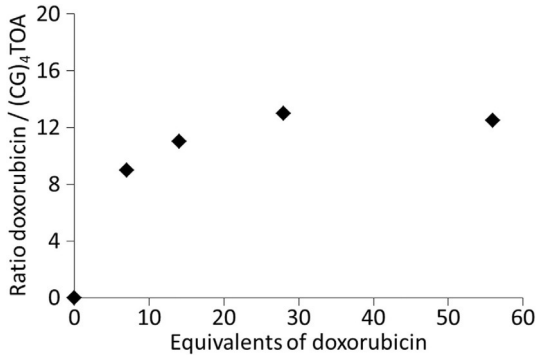

Figure 5. Inclusion of doxorubicin in the formulation with $(CG)_4TOA$ (**2**) at different ratios of API and hybrid. The molar ratio found in the solid is shown as a function of the equivalents of doxorubicin that were added to the hybrid solution at 37 °C.

Table 2. Formation of inclusion compounds from $(CG)_4TOA$ (**2**) and doxorubicin or imatinib from dilute aqueous buffer.[a]

API	API [equiv]	T_{mixing} [°C]	Hybrid precipitated [%]	Inclusion efficiency (molar ratio: API/hybrid)[b,c]
doxorubicin	14	70	>95	13:1
doxorubicin	14	50	>95	11:1
doxorubicin	14	37	>95	11:1
doxorubicin	14	22	>95	10:1
imatinib	15	70	60	20:1
imatinib	15	50	80	15:1
imatinib	15	37	95	6:1
imatinib	15	22	90	7:1
imatinib	8	37	50	9:1
imatinib	30	37	>95	6:1
imatinib	60	37	>95	7:1

[a] Conditions: 50 μM solution of **2**, 10 mM NH_4OAc, pH 7, mixing at the temperature listed and cooling to 22 °C within 12 h. [b] Doxorubicin was quantified by absorption at 487 nm, imatinib at 335 nm. [c] Depending on the temperature, imatinib initially gave an oily or glassy precipitate.

orubicin and imatinib. For either of the APIs, the temperature at which the hybrid and active ingredient were mixed was varied. Further, increasing molar equivalents of the API were used to test the saturation capacity of the carrier. Figure 5 and Table 2 show results from these experiments.

As with **1**, the uptake of the anthracycline reached saturation at ~13 equivalents over hybrid **2**. Because of the smaller mass of **2** (2.7 kDa) this means more than 70% percent of the dry weight of the preparation was API, ignoring counterions and solvation water. When 14 equivalents of the anthracycline were used, little of the API stayed unformulated in solution, and the precipitation of the hybrid was also near-quantitative (Table 2). The inclusion efficiency dropped modestly, to 10 equivalents, when the mixing was performed at room temperature, rather than 70 °C.

We then monitored the onset of complex formation between drug and carrier by temperature-dependent UV/Vis spectrophotometry. Wavelength scans at different temperatures confirmed that interactions between the aromatic chromophores of API and carrier can be detected by absorption spectroscopy in this case, as indicated by shifts in bands (Figures S15–S17, Supporting Information). Figure 6 shows the change of absorption at 260 nm upon cooling from 80 to 5 °C. When solutions of doxorubicin alone, carrier **2** alone, or a mixture of doxorubicin and linear control DNA strand $(dT)_8$ were cooled, no sigmoidal transition was observed (Figure 6a). The control experiment using linear DNA octamer $(dT)_8$ confirmed that the branched oligonucleotide hybrid has properties that are different from those of linear DNA with the same number of nucleotides. However, when solutions of doxorubicin and **2** were cooled, a new transition occurred that manifested itself in a flat region in the cold and a shift of the "UV-melting curve" to higher temperatures (Figure 6b). As expected for multimolecular complex formation, this shift in was strongly concentration dependent. While at 4 μM concentration of **2**, the onset of complex formation was at approx. 20 °C, the flattening of the curve set in at approx. 40 °C at 8 μM concentration of **2** under our experimental conditions. This monitoring technique may help to optimize formulations.

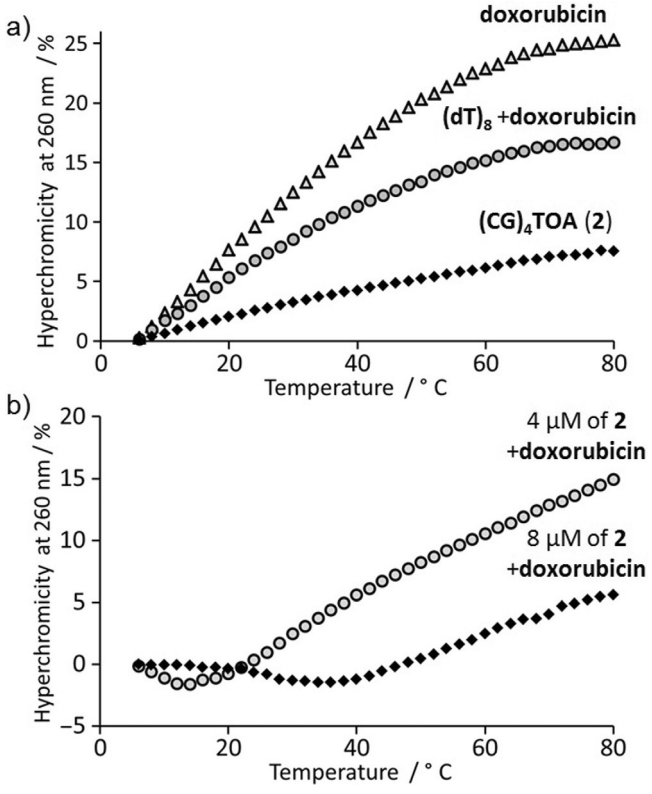

Figure 6. Studying complex formation between API and carrier by temperature-dependent UV absorption at 260 nm in 50 μM ammonium acetate buffer, pH 6.5, at a cooling rate of 1 °C min^{-1}. a) Control curves of solutions of $(CG)_4$TOA (**2**, 4 μM), doxorubicin (16 μM) and a mixture of linear DNA octamer $(dT)_8$ (4 μM) and doxorubicin (16 μM). b) Absorbance curves for solutions of $(CG)_4$TOA (4 μM or 8 μM) and doxorubicin (16 μM). Hyperchromicities are based on the absorbance at 5 °C.

For imatinib, the effect of temperature on encapsulation was even stronger than for doxorubicin, so that only a third of the exceptionally high inclusion efficiency found at 70 °C remained when API and carrier were mixed at 22 °C. The ratio of drug and carrier also changed to a less favorable ratio when the mixing was performed without heating. Increasing the amount of the drug at 37 °C led to near-quantitative precipitation of the hybrid, but the inclusion efficiency did not go up (Table 2). So, for this non-intercalating compound, a solubility equilibrium appears to exist that is reminiscent of those found for salts with their characteristic solubility product.

Inappropriate size and charge on carrier systems can lead to toxic side effects and rapid clearance from the circulation.[3] Therefore, we measured the size and ζ potential of particles formed when hybrid **2** as carrier and four representative APIs were mixed at 70 °C, followed by cooling. For this we chose doxorubicin, imatinib, mitoxantrone, and netropsin. Netropsin is an API that did not show signs of interactions with the monomeric form of the carrier, as indicated by UV-spectra acquired at different temperatures (Figures S18 and S19, SI). Imatinib is an API for which a particularly high encapsulation efficiency had been measured (Table 2). Among all drugs tested, mitoxantrone is the API that gave precipitates most readily upon mixing with the carrier, so that a certain breadth of drug structures was represented in these experiments. Table 3 lists the

Table 3. Size and ζ potential of nanoparticles formed from $(CG)_4$TOA (**2**) and various APIs in aqueous buffer.[a]

API	Average diameter [nm]	PDI[b]	ζ potential [mV][c]
doxorubicin	835	0.21	+8.2±3.9
imatinib	403	0.13	−18.0±3.4
mitoxantrone	114	0.01	+27.5±6.9
netropsin	525	0.04	−28.8±4.3

[a] Conditions: stock solutions of carrier in 10 mM NH_4OAc buffer, pH 7 and API (15 equiv) were mixed at 70 °C to give concentrations of 10 μM of **2** and 150 μM of the API, and then cooled to 22 °C in approx. 15 min, followed by size measurements via dynamic light scattering, and then dilution with water to 2.5 μM **2** and 37.5 μM API for measuring the ζ potential. [b] Polydispersity index. [c] Data are the mean ± standard deviation of 12 zeta runs. See Figures S20–S27 of the Supporting Information for further details.

size, as determined by dynamic light scattering (DLS), and the ζ potential for the different APIs. Plots and more detailed data can be found in the Supporting Information. Exploratory measurements by transmission electron microscopy also showed particles or small aggregates less than 1 μm in diameter (Figure S28, SI).

We then studied the release of APIs from the inclusion compounds. For this, the formulations obtained with the adamantane hybrid were layered with a volume of bovine serum at 37 °C, and the release of the drug without agitation of stirring was measured in the supernatant by UV/Vis spectrophotometry. Where the absorption of the serum was too strong to detect the API in the solution reliably, water was used instead. Figure 7 shows the release of doxorubicin, as measured for the formulation with **2** prepared at different mixing temperatures. As expected, the inclusion compound obtained at the lower mixing temperature released the drug most readily, whereas the higher temperature forms held on to the API more strongly. In either case, the amount released leveled off over the course of one day. The extent to which release occurred within 24 h for a number of different APIs and preparations was measured for the respective inclusion compounds, and the results are listed in Table 4.

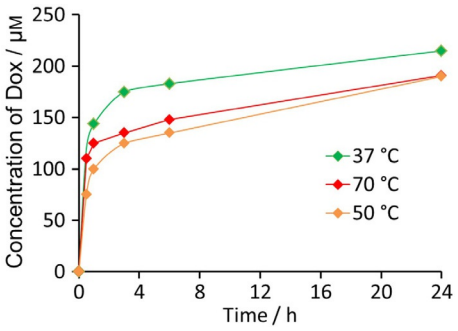

Figure 7. Release of doxorubicin from the solid formed with $(CG)_4TOA$ (**2**) during the first 24 h in fetal bovine serum at 37 °C, starting from inclusion compounds prepared with different mixing temperatures, as determined by UV/Vis absorption.

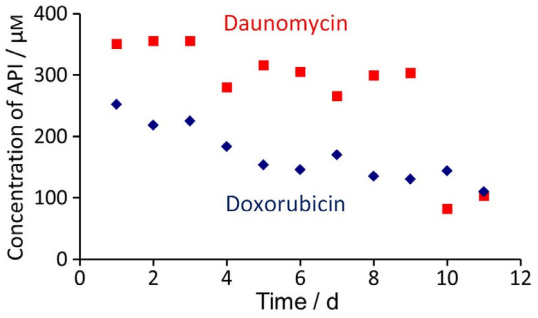

Figure 8. Release of daunomycin (red squares) or doxorubicin (blue rhombuses), into fetal bovine serum (FBS, 100 μL) from formulations with **1**, after 1 d at 37 °C without shaking. The concentrations of daunomycin and doxorubicin were determined by UV/Vis absorption. After each 24 h period, the sample was centrifuged and the serum was replaced with a new aliquot of FBS, followed by incubation at 37 °C for another 24 h. After 10 d, ~90% of the daunomycin and 50% of the doxorubicin were released from the solids.

The slowest release was measured for the anthracylines, prompting us to perform a long-term assay (Figure 8). For this, the supernatant was aspirated at the end of a 24 h period, and replaced with fresh serum, followed by renewed incubation at 37 °C without agitation or mixing. At the end of each period, the API content in the serum was measured and the process repeated. After ten days, the daunomycin inclusion compound was all but fully dissolved, leading to a sharp drop in what had been a fairly steady rate of release. For doxorubicin, the amount released per day was smaller, so that after 11 days, ap-

Table 4. Release of APIs from formulations with $(CG)_4TBA$ (**1**) or $(CG)_4TOA$ (**2**) into serum, as measured after 24 h.

Hybrid	API	Molar ratio: API/hybrid	Amount of API in preparation [nmol]	Medium[a]	API release after 24 h [nmol] (% of API)
1	daunomycin	8:1	400	FBS	35 (9)
1	doxorubicin	12:1	620	FBS	26 (4)
1	epirubicin	12:1	117	FBS[b]	10 (9)
1	proflavine	10:1	100	FBS[b]	24 (24)
1	mitoxantrone	5:1	50	FBS[b]	10 (20)
1	imatinib	8:1	84	H_2O	15 (18)
			69	FBS	55 (79)
1	tetracycline	5:1	38	H_2O	15 (40)
1	streptomycin	–	–	H_2O	n.d.[c]
1	methotrexate	1.2:1	180	H_2O[d]	35 (20)
1	gramicidin A	0.5:1	5	H_2O[e]	5 (quant.)
1	cyclosporin A	1:1	10	H_2O[e]	10 (quant.)
2	doxorubicin	13:1	130	FBS	19 (15)
2[f]	doxorubicin	11:1	110	FBS	22 (20)
2	imatinib	20:1	120	FBS	82 (68)
2[f]	imatinib	6:1	60	FBS	60 (quant.)

[a] Treated with 100 μL medium at 37 °C for 1 d, unless otherwise noted. [b] Treated with 200 μL. [c] Solid was treated with H_2O at 50 °C; streptomycin was detected by TLC. [d] Solid was treated at 50 °C for 15 min. [e] Solid was treated with 200 μL at 70 °C for 10 min and stored at 37 °C for 1 d, after which time it had dissolved quantitatively. [f] Inclusion compound had been prepared at a mixing temperature of 37 °C. All other inclusion compounds had been prepared at a mixing temperature of 70 °C.

proximately half of the formulation remained. At that time point, still more than a third of the quantity released during the first day was found in the supernatant after 24 h. That the hybrid matrix dissolved during the release process was confirmed by analyzing the supernatant in control assays with water, which allowed direct quantification of either component of the inclusion compound. Exploratory experiments with hybrids featuring longer DNA arms suggest that even larger quantities of anthracyclines can be encapsulated, and that even slower release from the hybridized networks can be achieved.

Conclusions

In conclusion, we show that adamantanes with four CG dimer appendages have the ability to form inclusion complexes with a broad range of different APIs, providing potential new formulations for a number of drugs that are on the WHO's list of Essential Medicines. While initially focused on DNA-binding drugs, our study showed that new inclusion compounds can also be formed with other APIs. For anthracyclines, the amount that is encapsulated far exceeds the two equivalents that would be expected for intercalation. Instead, a combination of intercalation and encapsulation in cavities formed by the hybrid lattice upon hybridization of the CG dimer arms is the most likely molecular scenario.

In recent years, an ever increasing number of biologics has been approved as active ingredients of pharmaceutical preparations. Here we show that a pruned-down version of a biological (an oligonucleotide) in combination with an adamantane core can be used to generate slow release formulations. As a biopolymer, DNA is biodegradable. For TOA hybrids, the remaining adamantane tetraol is an aliphatic alcohol that is unlikely to pose a toxicological problem. Further, the cost of our carriers is much lower than that of therapeutic oligonucleotides, because efficient solution-phase syntheses exists that are scalable and that use inexpensive, commercial starting materials.[28] With a loading capacity of up to 70% of the dry weight, the hybrids have the potential to become alternatives to established carriers for active pharmaceutical ingredients. Among the tasks that lay ahead are expanding the current work focused on molecular recognition and nanostructuring to biological studies. We are also working on approaches to expand this study into the realm of smart chemistry-based delivery,[33] as well as other forms of next generation nanomedicines, including those suitable for encapsulating biologics.

Experimental Section

General. The active pharmaceutical ingredients (APIs), fetal bovine serum (FBS) and water (Chromasolv for HPLC) were from Sigma Aldrich (Deisenhofen, Germany) or TCI Europe (Zwijndrecht, Belgium) and were used without further purification. The hybrids $(CG)_4$TBA (**1**) and $(CG)_4$TOA (**2**) were synthesized as described.[27,28] Thin layer chromatography (TLC) was performed with precoated silica gel sheets (SIL G/UV254 from Machery-Nagel) with visualization by ultraviolet light (254 nm) or staining. UV/Vis spectra were recorded using a ND-1000 spectrophotometer (NanoDrop; peQlab, Erlangen, Germany). For baseline correction, water or FBS was used as reference. MALDI-TOF mass spectra were acquired on a Bruker REFLEX IV spectrometer. The spectra were measured in linear negative mode using a matrix/comatrix mixture of 2,4,6-trihydroxyacetophenone (0.3 M in EtOH) and diammonium citrate (0.1 M in H_2O) at a ratio of 2:1 (*v*/*v*). Absorption spectroscopy was performed on a Lambda 25 spectrophotometer (PerkinElmer). Dynamic light scattering (DLS) data and ζ potential were measured with a Zetasizer Nano ZS90 system with 90° detector position. Transmission electron microscopy (TEM) was performed on an FEI Tecnai G2 electron microscope at an acceleration voltage of 200 kV.

Inclusion compounds of APIs with hybrids. The following protocol is representative and was used for all anthracyclines tested (daunomycin, doxorubicin and epirubicin), as well as proflavine, mitoxantone, netropsin and imatinib. A solution of $(CG)_4$TBA (**1**, 50 μL, 1 mM, 50 nmol) in NH_4OAc buffer (10 mM) was diluted with H_2O (50 μL) and heated to 70 °C for 15 min. A solution of doxorubicin (750 nmol, 15 equiv) in H_2O (100 μL) at 70 °C was added in one portion and the mixture was allowed to cool down to room temperature in a water bath during 12 h. The red solid formed was separated by centrifugation (16300 g, 2 min), the supernatant was aspirated and the solid was washed with water (100 μL). The supernatant was analyzed by UV/Vis measurement at 260 nm to determine the content of hybrid and, at the maximum of doxorubicin spectrum (487 nm), to determine the content of the API. Hybrid **1** was precipitated quantitatively (>95%); the ratio of doxorubicin/hybrid determined was 12:1. Further, a small sample of the solid (0.1 mg) was dissolved in H_2O/EtOH (300 μL, 2:1, *v*/*v* at 60 °C) and analyzed by MALDI-TOF MS. In the control assay lacking the hybrid, a solution of doxorubicin (200 μL, 150 μM; in NH_4OAc buffer 10 mM) was heated to 70 °C and cooled to room temperature over 12 h. The sample was centrifuged and analyzed by absorption measurement, as described above. When the same assay was repeated five times, the numerical value of the encapsulation efficiency was found to vary by less than 10% between the experiments.

Inclusion compounds of APIs with $(CG)_4$TBA with addition of $MgCl_2$. The following protocol was used for tetracycline, streptomycin, methotrexate, gramicidin A, cyclosporin A, actinomycin A and cytochrome c and is representative for encapsulation with addition of magnesium chloride. A solution of $(CG)_4$TBA (**1**, 10 μL, 1 mM, 10 nmol) in NH_4OAc buffer (10 mM) was diluted with H_2O (90 μL) and heated to 70 °C for 15 min. Then, a solution of methotrexate (150 nmol, 15 equiv) in H_2O (100 μL) at 70 °C was added in one portion and the mixture was allowed to cool to room temperature in a water bath over 12 h. After addition of $MgCl_2$ solution (2 μL, 1 M, 2 μmol, final concentration 10 mM), the mixture was vortexed for 10 s and then stored in the dark at room temperature for 24 h. The yellow precipitate was separated by centrifugation (16300 g, 2 min). The supernatant was aspirated and analyzed by UV/Vis measurement at 260 nm to determine the content of hybrid, and, at the maximum of the methotrexate spectrum (373 nm), to determine the concentration of the API. The hybrid was found to have precipitated to 90% of the initial amount, and the stoichiometric ratio of methotrexate/hybrid determined was 1:1. A control sample without the hybrid yielded no solid.

Release of anthracyclines into serum. The following protocol is representative and was used for all $(CG)_4$TBA inclusion compounds loaded with anthracyclines (daunomycin, doxorubicin, or epirubicin). A sample of the solid loaded with the anthracycline was prepared as described above. After centrifugation and washing with

water, the solid was treated with fetal bovine serum (FBS, 100 μL) without mixing or shaking, and was left standing at 37 °C in a temperature-controlled incubator oven. Samples of the supernatant (1 μL) were drawn at stated intervals and analyzed by UV-VIS absorption measurement. Absorption at the maxima of the anthracycline spectrum was used to determine the content of the anthracycline in the supernatant. After sampling, the remaining solid was separated by centrifugation (16300 g for 1 min), and fresh FBS (100 μL) was added, as described above, followed by incubation for another 24 h at 37 °C. This procedure was repeated daily for 12 d. The data points reported in Figures 7, Figure 8, and Table 4 are averages of three or four individual measurements that typically differed by less than 5%.

Monitoring by absorption spectroscopy. The following protocol is representative. It was used for monitoring the interactions of $(CG)_4$TOA (**2**) and doxorubicin. A solution of $(CG)_4$TOA (**2**, 4.9 μL, 0.83 mM, 4 nmol) in NH_4OAc buffer (10 mM, pH 6.5) was diluted with HPLC grade water to a final volume of 1 mL, followed by heating at 70 °C in a semimicro UV cuvette. Then, an aliquot of a stock solution of doxorubicin (1.0 μL, 16 mM, 16 nmol, 16 equiv) was added. The final concentrations in the solution were 4 μM **2** and 16 μM doxorubicin. The cuvette was heated to 70 °C to start measuring the temperature-dependent spectra (wavelength scans, Figures S15–S19, Supporting Information). For the measurements at 260 nm shown in Figure 6, samples that had cooled to 20 °C were briefly shaken and placed in a ultrasonic bath prior to heating again to 70 °C and acquisition of the absorption versus temperature curves.

Size measurement via dynamic light scattering. The following protocol is representative and was used for the mixture of $(CG)_4$TOA (**2**) and doxorubicin. A stock solution of $(CG)_4$TOA (**2**) in NH_4OAc buffer (10 mM) was diluted with H_2O (HPLC grade) to a volume of 100 μL and a concentration of 10 μM and was then heated to 70 °C. After addition of doxorubicin (final concentration 150 μM), the solution was transferred to a cuvette and placed in the Zetasizer. The final concentration of the NH_4OAc buffer was 100 μM. Two measurement runs were performed, leading to the results shown in Table 3 and Figures S20–S23 (SI).

Zeta potential of particles. A stock solution of $(CG)_4$TOA (**2**) in NH_4OAc buffer (10 mM) was diluted with H_2O to a volume of 100 μL, resulting in a concentration of 20 μM **2**, followed by heating at 70 °C, addition of doxorubicin (15 equiv), cooling to 25 °C, and dilution to a final volume of 800 μL with water. The final concentrations were 2.5 μM $(CG)_4$TOA, 37.5 μM doxorubicin, and 30 μM NH_4OAc buffer. The capillary cell was prepared by rinsing with ethanol (20 mL) and water (10 mL). The sample solution (0.8 mL) was placed in the capillary cell and inserted into the Zetasizer, leading to the results shown in Table 3 and in Figures S24–S27 (ζ potential).

Transmission electron microscopy. A solution of **2** (100 μM, 100 μL) was heated to 80 °C, cooled to 50 °C in 2 h, and treated with doxorubicin (4 equiv), followed by cooling to 20 °C in 8 h, resulting in a reddish precipitate. The mixture was vortexed for 10 s and a sample was placed on a copper grid (coated with carbon, Plano Wetzlar). After 5 min, excess liquid was removed from the grid using a filter paper. Then, uranyl formiate (5 μL, 1% in H_2O) was added and immediately removed by capillary forces with filter paper. This procedure was repeated once, with removal of excess uranyl formiate solution after 20 s. The grid was dried and used for electron microscopy.

Supporting Information. Representative spectra of starting materials, inclusion compounds and samples from the drug release assay can be found in the Supporting Information.

Acknowledgements

The authors thank Th. Sabirov and D. Göhringer for technical assistance, Tanja Walter for acquisition of UV/Vis spectra, Rainer-Joachim Schwarz for help with TEM measurements, CureVac AG (Tübingen) for access to a Zetasizer, and Dr. C.-P. Niesert for discussions. This work was supported by DFG (grant No. RI 1063/15-1 to C.R.).

Conflict of interest

The authors declare no conflict of interest.

Keywords: adamantane · anthracyclines · controlled release · DNA hybrids · formulation

[1] M. W. Tibbitt, J. E. Dahlman, R. Langer, *J. Am. Chem. Soc.* **2016**, *138*, 704–717.
[2] J. Ding, L. Chen, C. Xiao, L. Chen, X. Zhuang, X. Chen, *Chem. Commun.* **2014**, *50*, 11274–11290.
[3] C. Wan, T. M. Allen, P. R. Cullis, *Drug Delivery Transl. Res.* **2014**, *4*, 74–83.
[4] D. Luo, W. M. Saltzman, *Nat. Biotechnol.* **2000**, *18*, 33–37.
[5] J. W. de Vries, F. Zhang, A. Herrmann, *J. Controlled Release* **2013**, *172*, 467–483.
[6] J. Chao, H. Liu, S. Su, L. Wang, W. Huang, C. Fan, *Small* **2014**, *10*, 4626–4635.
[7] V. Linko, A. Ora, M. A. Kostiainen, *Trends Biotechnol.* **2015**, *33*, 586–594.
[8] J. Yan, C. Hu, X. Liu, J. Zhong, G. Sun, D. He, *Curr. Pharm. Des.* **2015**, *21*, 3181–3190.
[9] R. B. Weiss, *Semin. Oncol.* **1992**, *19*, 670–686.
[10] G. Minotti, P. Menna, E. Salvatorelli, G. Cairo, L. Gianni, *Pharmacol. Rev.* **2004**, *56*, 185–229.
[11] M. Wilhelm, A. Mukherjee, B. Bouvier, K. Zakruewska, J. T. Hynes, R. Lavery, *J. Am. Chem. Soc.* **2012**, *134*, 8588–8596.
[12] M. Davenport, *Chem. Eng. News* **2014**, *92*, 10–13.
[13] D. J. Taatjes, D. J. Fenick, T. H. Koch, *J. Med. Chem.* **1998**, *41*, 1306–1314.
[14] R. Toita, M. Murata, K. Abe, S. Narahara, J. S. Piao, J.-H. Kang, M. Hashizume, *Chem. Commun.* **2013**, *49*, 7442–7444.
[15] P. Horcajada, T. Chalati, C. Serre, B. Gillet, C. Sebrie, T. Baati, J. F. Eubank, D. Heurtaux, P. Clayette, C. Kreuz, J.-S. Chang, Y. K. Hwang, V. Marsaud, P.-N. Bories, L. Cynober, S. Gill, G. Ferey, P. Couvreur, R. Gref, *Nat. Mater.* **2010**, *9*, 172–178.
[16] T. Etrych, P. Chytil, M. Jelinkova, B. Rihova, K. Ulbrich, *Macromol. Biosci.* **2002**, *2*, 43–52.
[17] L. Purdie, C. Alexander, S. G. Spain, J. P. Magnusson, *Bioconjugate Chem.* **2016**, *27*, 1244–1252.
[18] Y. X. Zhao, A. Shaw, X. Zeng, E. Benson, A. M. Nyström, B. Högberg, *ACS Nano* **2012**, *6*, 8684–8691.
[19] P. D. Halley, C. R. Lucas, E. M. McWilliams, M. J. Webber, R. A. Patton, C. Kural, D. M. Lucas, J. C. Byrd, C. E. Castro, *Small* **2016**, *12*, 308–320.
[20] C. Ducani, C. Kaul, M. Moche, W. M. Shih, B. Högberg, *Nat. Methods* **2013**, *10*, 647–652.
[21] P. W. K. Rothemund, *Nature* **2006**, *440*, 297–302.
[22] F. C. Simmel, *Front. Life Sci.* **2012**, *6*, 3–9.
[23] M. Meng, C. Ahlborn, M. Bauer, O. Plietzsch, S. A. Soomro, A. Singh, T. Muller, W. Wenzel, S. Bräse, C. Richert, *ChemBioChem* **2009**, *10*, 1335–1339.
[24] A. Singh, M. Tolev, M. Meng, K. Klenin, O. Plietzsch, C. I. Schilling, T. Muller, M. Nieger, S. Braese, W. Wenzel, C. Richert, *Angew. Chem. Int. Ed.* **2011**, *50*, 3227–3231; *Angew. Chem.* **2011**, *123*, 3285–3289.

[25] A. Schwenger, C. Gerlach, H. Griesser, C. Richert, *J. Org. Chem.* **2014**, *79*, 11558 – 11566.
[26] H. Griesser, M. Tolev, A. Singh, T. Sabirov, C. Gerlach, C. Richert, *J. Org. Chem.* **2012**, *77*, 2703 – 2717.
[27] A. Singh, M. Tolev, C. Schilling, S. Bräse, H. Griesser, C. Richert, *J. Org. Chem.* **2012**, *77*, 2718 – 2728.
[28] A. Schwenger, N. Birchall, C. Richert, *Eur. J. Org. Chem.* **2017**, DOI: https://doi.org/10.1002/ejoc.201700686.
[29] K. Spilovska, F. Zemek, J. Korabecny, E. Nepovimova, O. Soukup, M. Windisch, K. Kuca, *Curr. Med. Chem.* **2016**, *23*, 3245 – 3266.
[30] T. H. Maugh, *Science* **1979**, *206*, 1058 – 1060.
[31] E. A. Govorkova, H.-B. Fang, M. Tan, R. G. Webster, *Antimicrob. Agents Chemother.* **2004**, *48*, 4855 – 4863.
[32] A. A. Spasov, T. V. Khamidova, L. I. Bugaeva, I. S. Morozov, *Pharm. Chem. J.* **2000**, *34*, 1 – 7.
[33] T. Ramasamy, H. B. Ruttala, B. Gupta, B. K. Poudel, H. G. Choi, C. S. Yong, J. O. Kim, *J. Controlled Release* **2017**, *258*, 226 – 253.

Manuscript received: August 7, 2017
Revised manuscript received: September 6, 2017
Accepted manuscript online: September 15, 2017
Version of record online: October 9, 2017

